In-line digital holographic interferometry

Giancarlo Pedrini, Philipp Fröning, Henrik Fessler, and Hans J. Tiziani

An optical system based on in-line digital holography for the evaluation of deformations is described. In-line holograms are recorded on a CCD chip. The problem of overlapping twin images typical for the in-line arrangement is solved by digital reconstruction and filtering of the unwanted wave fronts. Two separate interferograms of an object under test in its undeformed and deformed states are recorded each on a CCD chip. The phases of the two wave fronts are obtained from the complex amplitudes of the digital reconstructed wave fronts, and the deformation is calculated from the phase differences. Experimental results are presented. © 1998 Optical Society of America

OCIS codes: 070.0070, 070.2580, 070.2590, 090.0090, 090.1760, 090.2880, 100.0100, 100.2000, 100.2650.

1. Introduction

Holographic techniques permit the measurement of displacements and deformations without contact.[1,2] Traditionally, photographic films were used to record the holograms. Photographic films have a very high resolution (e.g., 5000 line pairs/mm) but have the disadvantage that they need wet chemical development. After recording a hologram on such films, a physical reconstruction of the recorded wave field by illumination of the photographic plate with a laser is needed. The procedure is time consuming.

Computer capacities and the spatial resolution of CCD sensors (CCD's with more pixels and a reduced pixel size) increase constantly. Thus it is now possible to record a hologram (interference between a object and its reference) by use of a CCD and to evaluate it digitally. This technique is better suited to an industrial environment than are photographic films. The resolution of the sensor must be sufficient to record the fringes formed by the reference wave and the wave coming from the object. The maximum spatial frequency, which can be recorded with a CCD camera, is limited by the pixel size.

Different arrangements for digital holography are possible: Some use a lens to image the object on the CCD.[3] This technique is sometimes called speckle interferometry with a spatial carrier. For evaluation a Fourier method[4] can be used. Another possibility is to record, without use of a lens, a Fourier or a Fresnel hologram on a CCD chip.[5,6] For a Fresnel hologram the arrangement is the same as that used to record a classical off-axis hologram. It is only necessary to take care that the angle between the object and the reference beams is small enough (typically a few degrees) to allow the CCD to record the fringes. Reconstruction occurs by simulation of the wave field diffracted by the hologram. The phases of the two reconstructed wave fields, which are recorded at different times, are calculated from the complex amplitude, and the deformation is obtained from the phase difference of the two wave fields.

All the above-described methods for digital holography use an off-axis reference and the digital reconstructed images are spatially separated. In early holography (see, e.g., Ref. 7, Chap. 2), an in-line arrangement was used. The in-line arrangements have the disadvantage that during reconstruction two overlapping twin images are obtained—one unfocused conjugate image overlaps the focused image. Because of this disadvantage the arrangement can be used in only a few applications. In Ref. 8 a method is described that is based on in-line digital holography for particle-size and -position measurements. Reference 9 describes a method for the reconstruction of in-line holograms. The method works only when the wave fields are produced by objects that can be described by a set of two-dimensional (2-D) real-valued opacity functions.

In this paper we show how the in-line arrangement can be used when the hologram is recorded on a CCD chip. In this case the hologram is not physically reconstructed, but the reconstruction is done digitally

The authors are with the Institut für Technische Optik, Universität Stuttgart, Pfaffenwaldring 9, D-70569 Stuttgart, Germany.

Received 5 December 1997; revised manuscript received 12 May 1998.

0003-6935/98/266262-08$15.00/0

© 1998 Optical Society of America

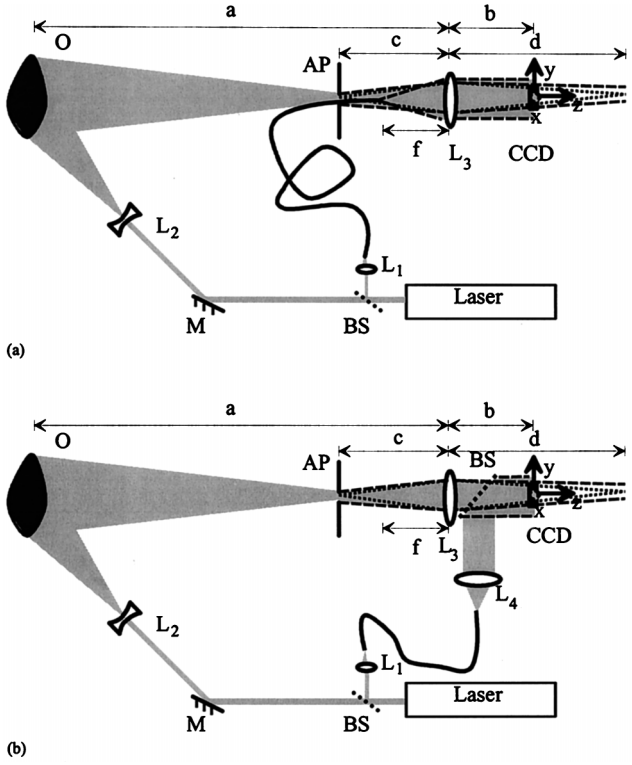


Fig. 1. Schematic of the experimental arrangements for in-line digital holographic interferometry. The reference beam is coupled into the interferometer by use of (a) fiber or (b) a beam splitter.

by use of a computer. The digital manipulation of the wave fronts permits the separation of the desired from the unwanted reconstructions. A pulsed ruby laser is used for our investigations.

2. In-Line Digital Holographic Interferometry

A. Recording of the In-Line Digital Hologram on a Charge-Coupled Device Sensor

Two schematics of the setup used for recording in-line holograms are shown in Fig. 1. Consider first the arrangement shown in Fig. 1(a). The laser beam is split into two by a beam splitter (BS). One of these two beams illuminates the object; the other is used as a reference. The illuminated object is imaged by lens L_3 onto a CCD sensor. An aperture (AP) in front of the lens can be used to control the speckle size in the image plane. The distance between the aperture and the lens is c. To convey the reference beam, we used a monomode optical fiber, making the arrangement more compact. A reference point source can be produced by passage of a thin optical fiber through the aperture. The fiber end is located on the axis in the front focal plane of the lens. Lens L_3 transforms the reference point source emerging from the fiber end into a plane wave that propagates along the z axis.

We consider a homogeneous plane reference wave. In the CCD plane, we can write the plane homogeneous reference wave r and the object wave u in the following form:

$$r(x, y) = A \exp(i\phi_R), \qquad |r(x, y)| = A = \text{const}, \quad (1a)$$

$$u(x, y) = |u(x, y)|\exp[i\phi(x, y)]. \quad (1b)$$

The intensity recorded by the CCD sensor is given by

$$I = |r(x, y)|^2 + |u(x, y)|^2 + r(x, y)u^*(x, y) + r^*(x, y)u(x, y) \quad (2a)$$

$$= A^2 + |u(x, y)|^2 + 2A|u(x, y)|\cos[\phi(x, y) - \phi_R], \quad (2b)$$

where the asterisk denotes complex conjugation and ϕ_R is the constant phase of the reference beam that we assume is equal to 0; thus $r(x, y) = r^*(x, y) = A$.

The maximum spatial frequency to be recorded is limited by the resolution of the CCD, i.e., a pixel size Δ of the photosensors. At some points the spatial frequency can exceed the resolution of the CCD. From the sampling theorem we know that, for recording of a hologram, it is necessary to have at least two sampled points for each fringe. This means that the change in phase from one pixel to the adjacent one should be smaller than π. To determine at which position we need to locate the aperture to allow the recording of the hologram, we consider first a case in which the object wave is a spherical wave emerging from a point located at the center of an aperture. This point source is imaged onto the plane $z = (d - b)$. In plane $z = 0$ (the CCD plane), this converging spherical wave can be written in the form

$$u(x, y) = B \exp\left[-\frac{\pi i}{\lambda}\frac{(x^2 + y^2)}{(d-b)}\right], \quad (3)$$

where λ indicates the wavelength and B the amplitude of the wave. By substituting Eq. (3) into Eq. (2), we obtain the relation

$$I(x, y) = A^2 + B^2 + 2AB \cos\left[\frac{\pi}{\lambda}\frac{(x^2 + y^2)}{(d - b)}\right], \quad (4)$$

which describes the intensity produced by the interference between a spherical and a plane wave. The fringe density increases radially from the hologram center. In the plane of the CCD we replace x with $N_x\Delta$ and y with $N_y\Delta$ (where N_x and N_y are integer numbers and Δ is the pixel spacing). The change of phase from one pixel (N_x, N_y) to the next $(N_x + 1, N_y + 1)$ should be less than π. This condition can thus be written in the form

$$\left[\frac{\pi}{\lambda}\frac{1}{(d - b)}\right]\{[(N_x + 1)\Delta]^2 + [(N_y + 1)\Delta]^2 - (N_x\Delta)^2 + (N_y\Delta)^2\} < \pi, \quad (5)$$

and after some simplification we have

$$(d - b) \geq \left(\frac{1}{\lambda}\right)[(2N_x + 2N_y + 2)\Delta^2]. \quad (6)$$

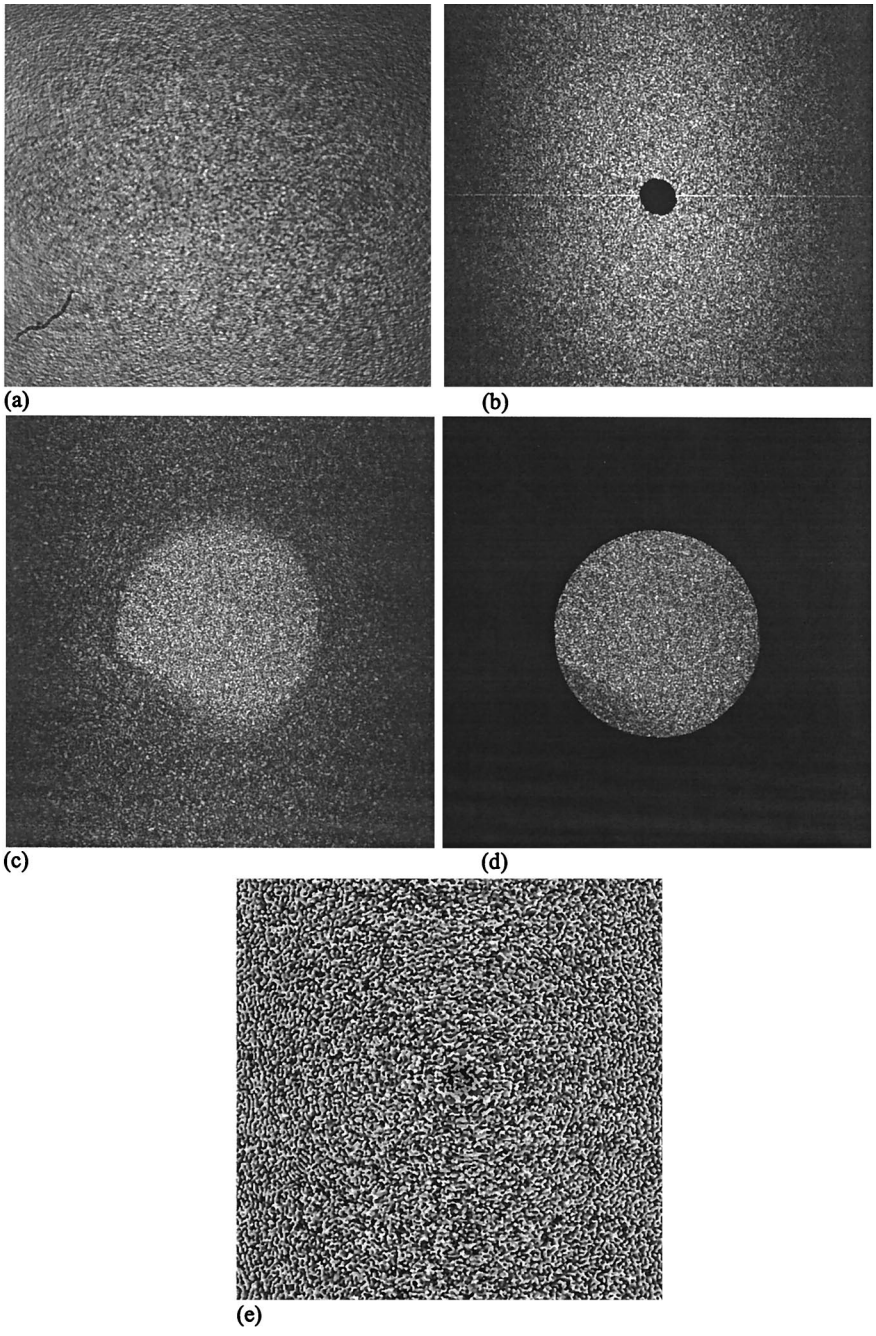


Fig. 2. Method used for the suppression of the unwanted reconstruction: (a) digitally sampled in-line hologram recorded on a CCD, (b) absolute value of the Fourier transform of a hologram with a high-pass filter for the suppression of the dc term, (c) digital reconstruction of the image of the aperture, (d) filtering of the image to remove the noise, and (e) phase of the wave front.

If condition (6) is not satisfied for each point of the hologram, undersampling occurs. Relation (6) tells us at what distance from the lens the aperture should be located to allow the recording of a well-sampled hologram on a $2N_x \times 2N_y$ CCD chip (pixel spacing of Δ).

If the object wave is not a point source, the wave field can be seen as a superposition of spherical waves emerging from different points of the aperture and converging on the aperture image plane $z = (d - b)$. For recording one hologram the CCD should be able to record the maximal spatial frequency that is due to the interference between the object and the reference waves. We will have speckle in the plane of the CCD because of the superposition of spherical waves converging from different points to the same points. The speckle size is a function of the aperture size. If the aperture is small, we have large speckle; if the aperture is large, the speckle is small.

Figure 2(a) shows an intensity pattern recorded on a CCD chip by use of the arrangement shown in Fig. 1(a). The pattern has a size of $2N_x \times 2N_y = 512 \times$

512 pixels. A pulsed ruby laser was used (wavelength of 694 nm). The distance between the object and lens L_3 was 1100 mm. The focal length of lens L_3 was $f = 60$ mm. For an aperture with a diameter of $D = 1.8$ mm located at a distance of $c = 80$ mm from the lens, using the lens formula shows b and d to be 63 and 240 mm, respectively. The pixel size was $\Delta = 11$ μm. The arrangement was chosen to satisfy relation (6): $(d - b) = 177$ mm $= (512 + 512 + 2)(11^2/694)$ mm. Because the reference and the object beams do not have the same divergence, the interferogram recorded on the CCD [Fig. 2(a)] has a radial symmetry. In the center, we have only low and at the border high carrier frequencies. For recording it is possible to use the arrangement described in Fig. 1(b) as well, where the reference is coupled into the interferometer by use of the beam splitter. The arrangement shown in Fig. 1(a) is more compact, and no beam splitter is needed.

B. Reconstruction of the In-Line Digital Hologram

For our application we are interested in determining the phase of the wave front u. From the recorded intensity [Eq. (2)] we cannot determine directly the phase $\phi(x, y)$. The first step is to eliminate the term $A^2 + |u(x, y)|^2$. We can do this by performing a Fourier transform and filtering in the Fourier plane, followed by an inverse Fourier transform. The Fourier transform is calculated by means of a computer. Figure 2(b) shows the filtering operation, for which a high-pass filter is applied (only the absolute value of the Fourier transform is shown). After the filtering operation the pattern is inversly transformed and a wave field is obtained that can be described by

$$H(x, y) = v(x, y) + Au^*(x, y) + Au(x, y), \qquad (7)$$

where $v(x, y)$ describes the residual wave field remaining after the Fourier filter is applied to $|u(x, y)|^2$. It is not possible to eliminate this term completely without eliminating $Au^*(x, y) + Au(x, y)$ because it contains low and high frequencies. This residual term will introduce noise by the determination of the phase.

If we suppose a value of $v(x, y) = 0$, then we get $H(x, y) = A[u^*(x, y) + u(x, y)]$, which describes the superposition of the object wave fronts (converging wave front) and its conjugate (diverging) wave front. We have here an in-line arrangement; hence the two wave fields are not spatially separated. To separate one from the other, we simulate the propagation of the wave fronts. This can be done by simulation of the Fresnel diffraction, as described in Refs. 5 and 6. In particular, we calculate the wave front in the plane $z = (d - b)$. Figure 2(c) shows the absolute value of the reconstructed wave front in this plane along with a digitally reconstructed image of the aperture. The image of the aperture is not perfectly circular; in particular, at the bottom left-hand side there is a shadow that is produced by the optical fiber's (diameter of 125 μm) passing through the aperture. Reconstructing the wave front from the hologram means that the size of the digitally reconstructed wave field at the distance z will have the dimension $L \times L$, where $L = \lambda z/\Delta$. In the example shown in Fig. 2(c), where $z = 177$ mm, the size of the wave field is $L \times L = 11.2$ mm $\times$ 11.2 mm. The diameter of the reconstructed image of the aperture shown in Fig. 2(c) is $D_i = 5.4$ mm $= M \times D$, where the value $M = d/c = 3$ is the magnification of the lens and the value $D = 1.8$ mm is the size of the aperture (AP). This example shows that the image of the aperture can be digitally reconstructed only when D_i is smaller than L. Throughout this image it is possible to see the noise produced by the reconstruction of the conjugate twin image. During recording the aperture and the reference point source were located in different planes. For this reason, when one of the two reconstructed twin wave fronts produces a focused image of the aperture in plane $z = (d - b)$, the other wave front produces a defocused image. The conjugated (defocused) wave front seems to diverge from one image of the aperture located in plane $z = -(d - b)$.

The noise outside the image of the aperture is filtered out, as shown in Fig. 2(d). After filtering, when at least a large part of the conjugate wave front is eliminated, we simulate backpropagation in the plane of the hologram ($z = 0$). This can be described by

$$H_1(x, y) = v(x, y) + w(x, y) + Au(x, y). \qquad (8)$$

We are interested in only the phase of the wave field $u(x, y)$. The wave fields $v(x, y)$ and $w(x, y)$ are residual parts that are the result of filtering the terms $|u(x, y)|^2$ and $Au^*(x, y)$, respectively, which introduces noise in the calculated phase. The phase is calculated according to

$$\phi(x, y) = \arctan \frac{\mathrm{Im}[u(x, y)]}{\mathrm{Re}[u(x, y)]} \approx \arctan \frac{\mathrm{Im}[H_1(x, y)]}{\mathrm{Re}[H_1(x, y)]}. \qquad (9)$$

Figure 2(e) shows the wrapped phase of the wave front calculated by use of expression (9) and having values between $-\pi$ and π.

Another possibility for obtaining the phase of the wave front is to use the conjugate reconstruction. In particular, after the reconstruction of the image of the aperture [Fig. 2(c)], we apply a high-pass filter [the complement of that shown in Fig. 2(d)] that filters out the image of the aperture. After the filtering operation, we simulate backpropagation in the plane of the hologram ($z = 0$). This can be described by

$$H_2(x, y) = v'(x, y) + Au_r^*(x, y). \qquad (10)$$

The wave field $v'(x, y)$ is the residual part of the imperfect filtering of the term $|u(x, y)|^2$, and $Au_r^*(x, y)$ is the remaining part of the conjugate wave front $Au^*(x, y)$ after filtering. Because $|v'(x, y)| \ll$

$|Au_r^*(x, y)|$, we neglect $v'(x, y)$ and calculate the phase from

$$\phi_r(x, y) = \arctan \frac{\mathrm{Im}[u_r^*(x, y)]}{\mathrm{Re}[u_r^*(x, y)]} \approx \arctan \frac{\mathrm{Im}[H_2(x, y)]}{\mathrm{Re}[H_2(x, y)]}. \tag{11}$$

It is particularly important to know the size of aperture needed to obtain a good determination of the phase. If we choose a large aperture, the overlap between the image of the aperture and the reconstructed conjugate field will be larger; therefore the filtering is less efficient. This will produce results of a lower quality. On the other hand, the aperture should be chosen to be as large as possible to have a better spatial resolution and collect more light. We obtained a good result in our experiments by choosing the size of the aperture to obtain the pattern as shown in Fig. 2(c), for which the diameter of the image of the aperture is approximately half the size of the total reconstructed pattern. More on the influence of the aperture size is reported in Section 3.

C. Calculation of the Deformation by Phase Subtraction

When the object is deformed the phases $\phi(x, y)$ and $\phi_r(x, y)$ change as functions of the deformation. We recorded two digital holograms before and after deformation. First, let us consider the change of phase of the reconstructed wave front. If $\phi(x, y)$ and $\phi'(x, y)$ are the phases before and after deformation, respectively, the phase difference $\Delta\phi(x, y) = \phi'(x, y) - \phi(x, y)$ contains information concerning the deformation. The phases $\phi(x, y)$ and $\phi'(x, y)$ calculated by use of expression (9) vary between $-\pi$ and π. To obtain a phase difference $\Delta\phi(x, y)$ in the interval between 0 and 2π, we added 2π if $\Delta\phi(x, y) < 0$. The phase map obtained in this manner contains a 2π incertitude that can be removed by means of phase unwrapping. The relation between the unwrapped phase $\Delta\phi_u$ and the deformation $\mathbf{d}$ is given by

$$\Delta\phi_u = \frac{2\pi}{\lambda} \mathbf{ds}, \tag{12}$$

where $\mathbf{s}$ is the sensitivity vector given by the geometry of the setup. The dependence on (x, y) has been omitted for convenience.

Analogously, we can calculate the phase difference in the conjugated wave field. The terms ϕ_r and ϕ_r' are the phases of the conjugated wave field before and after, respectively, the deformation, and the phase difference is $\Delta\phi_r = \phi_r' - \phi_r$. If we could completely separate the primary and the conjugate reconstructions, we would have $\phi = -\phi_r$, $\phi' = -\phi_r'$, and $\Delta\phi = -\Delta\phi_r$. The separation is not perfect, as we saw in Subsection 2.B, and the relation is only approximately satisfied.

3. Experimental Results

Figure 3 shows the experimental results obtained by use of a plate that was deformed between two exposures. The size of the plate was 50 mm × 50 mm. Two holograms were recorded on a CCD. Figure 3(a) shows the fringes produced by subtraction between the two digital holograms (subtraction of the intensities). The contrast of the fringes at the center of the image is better than at the borders. We saw above that, at the center of the image, the reference and the object waves have almost the same curvature. This means that the interference between these two waves will produce only low spatial frequencies. At the border the speckle is modulated with higher spatial frequencies, and this reduces the visibility.

The fringes shown in Fig. 3(a) do not contain the information on the phase change and do not permit a quantitative evaluation. The phase can be calculated by use of the method described above. Figure 3(b) shows a phase map obtained by subtraction of the two phases recorded before and after deformation. It is apparent that, at the center of the phase map, the quality of the image is not good. This is because during the filtering procedure part of the low spatial frequencies (at the center of the image) was eliminated by filtering of the dc term in the Fourier plane. This causes a decrease in the quality of the phase map. The phase map shown in Fig. 3(c) was obtained by use of the conjugate-reconstruction method. It is apparent that (on average) the phases shown in Fig. 3(c) have a negative sign with respect to the phase shown in Fig. 3(b). At the center the quality of the phase map shown in Fig. 3(c) is better compared with that shown in Fig. 3(b). For the conjugate method, we use a high-pass filter and the corresponding phase map contains high-frequency noise.

Figure 4 shows another example in which a plate vibrating at a frequency of 1295 Hz was investigated. For the measurement of quasistatic or slow deformation it is possible to record the holograms with a cw laser. For the measurement of dynamic events (e.g., shock or vibrations) it is necessary to use a pulsed laser. The pulse length of a ruby laser is approximately 50 ns; this allows us to freeze the movement of the object. Two holograms were recorded with the arrangement shown in Fig. 1(b) with the reference coupled into the interferometer by use of a beam splitter. The position of the aperture and the focal length of the lens were the same as in the experiment above. The aperture size is increased. Figure 4(a) shows the reconstructed image of the aperture. The diameter is approximately 1.5 times larger than that used above. Figures 4(b) and 4(c) show the phase maps obtained by use of the primary and the conjugate wave fronts, respectively. The noise level is increased with respect to Fig. 3, but the phase maps are still of good quality.

In Figs. 4(b) and 4(c) it is possible to see that, when the quality of one phase map is good, the quality of the other is not so good. To explain this behavior, we looked at the intensity of the object wave front and noticed its inhomogenity. In particular, regions where the object wave front is strong correspond to

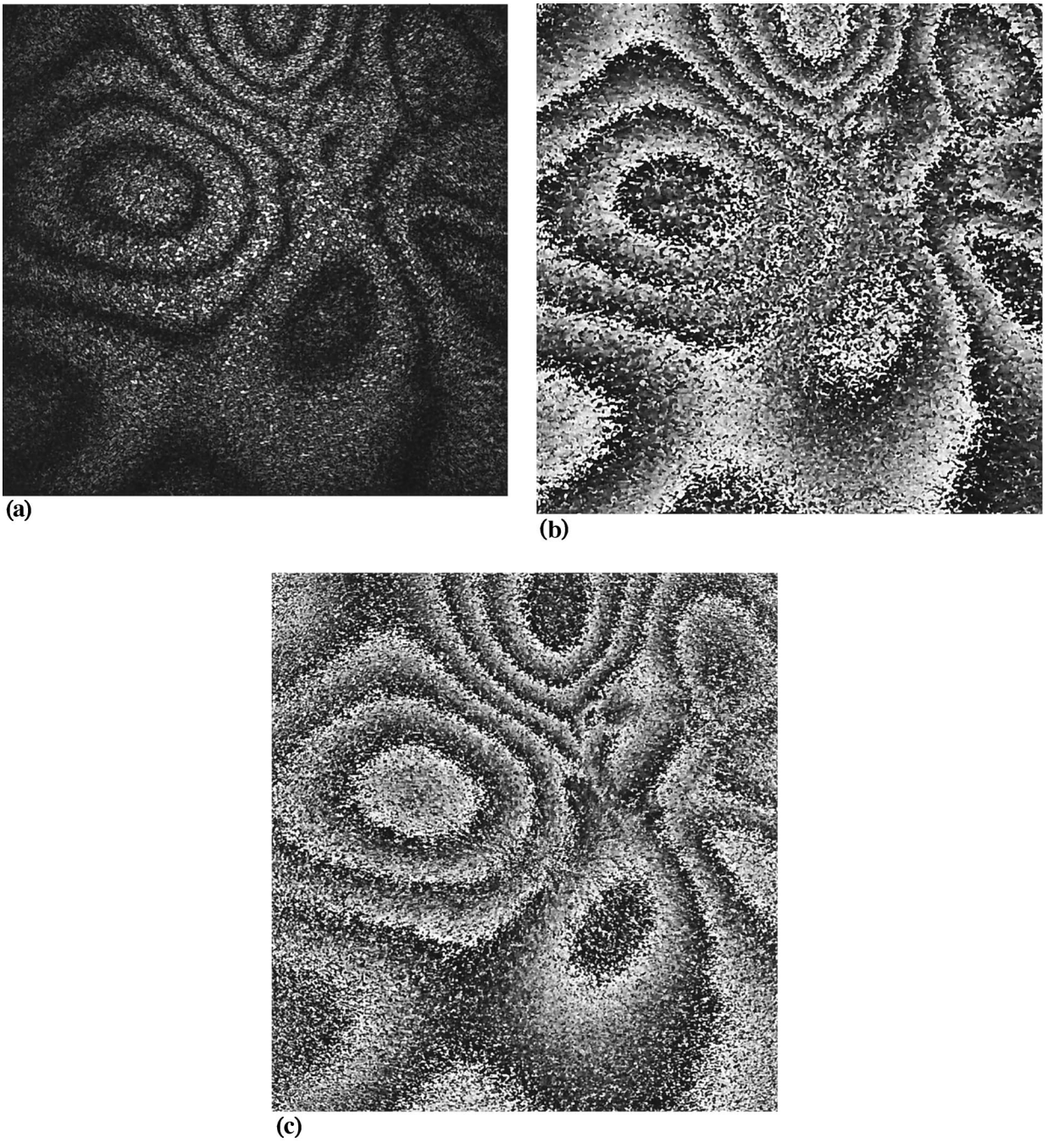


Fig. 3. Experimental results obtained by the deformation of a metallic plate: (a) Fringes obtained by subtraction the intensities of the two holograms. Phase maps obtained by (b) primary reconstruction and (c) conjugated reconstruction.

the surfaces of poor quality in Fig. 4(b). This noise is produced by the term $|u(x, y)|^2$ [present in Eq. (2)]; as was pointed out above, this term cannot be eliminated completely by the filtering operation. This term (noise in the phase map) is strong when the object wave front is strong and contains spatial frequencies that are strong for low frequencies and weak for high frequencies [the Fourier transform of this term is FT $[u(x, y)] \otimes$ FT $[u^*(x, y)]$, where the symbol $\otimes$ denotes convolution. In the conjugated phase map the noise is stronger when the object wave front is weaker; in this case it is not the term $|u(x, y)|^2$ that is responsible for the noise (this term does not contain strong high spatial frequencies) but just the fact that the object wave front is too weak with respect to the reference beam to produce high-spatial-frequency interference fringes with good contrast. For a quantitative evaluation it is possible to combine the primary and the conjugated phase maps and use the one with less noise. Figure 4(d) shows a pseudo 3-D representation of the deformation obtained after unwrapping the phase maps.

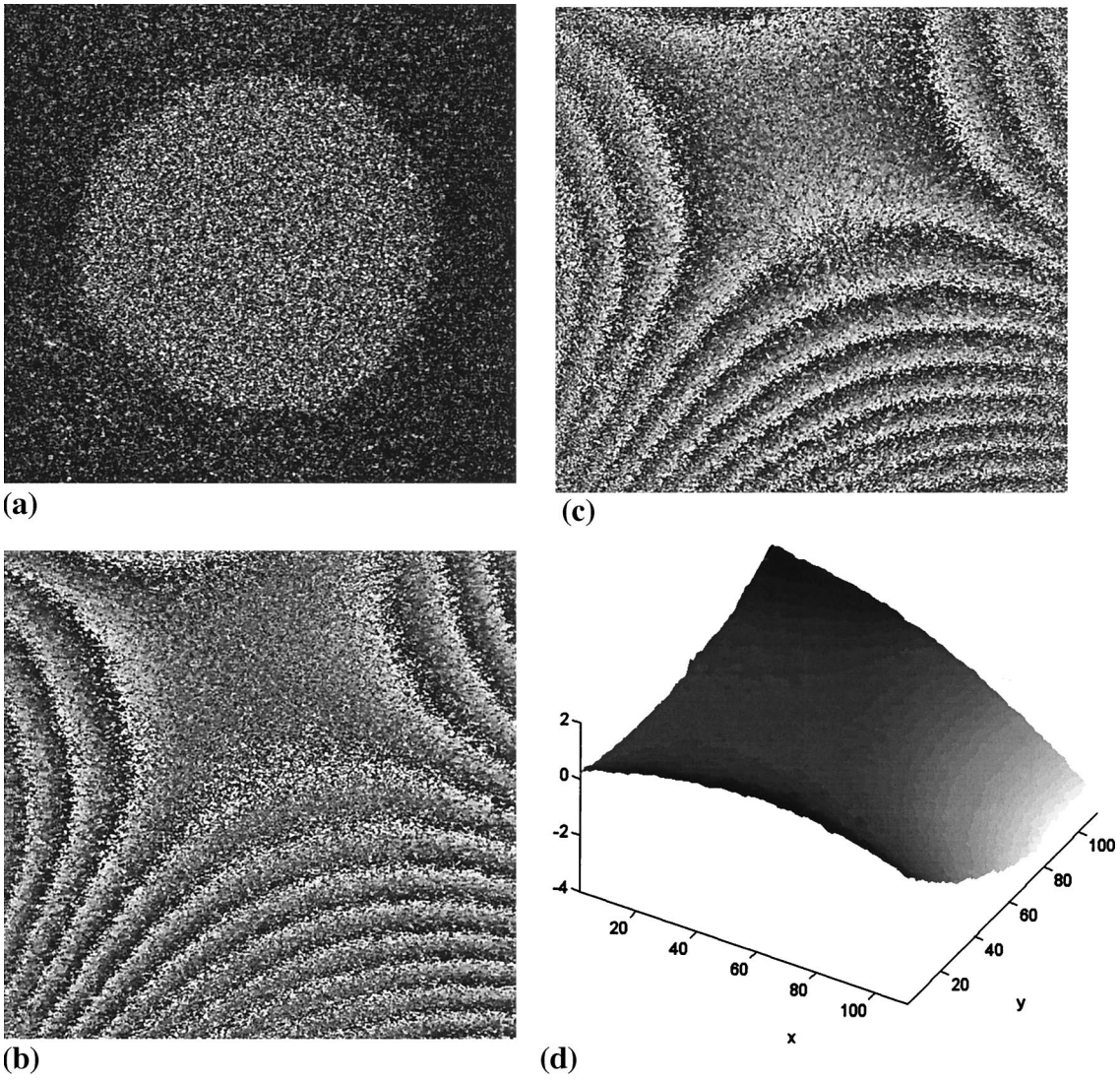


Fig. 4. Plate vibrating with a frequency of 1295 Hz. (a) Digital reconstruction of the image of the aperture. (b) Phase maps obtained by primary reconstruction. (c) Phase maps obtained by conjugated reconstruction. (d) Pseudo 3-D representation of the deformation.

4. Discussion and Conclusions

The digital holographic interferometry system described in this paper permits the quantitative analysis of in-line recorded digital holograms. We have shown how twin reconstruction can be eliminated by filtering the digitally reconstructed wave fields. The phase corresponding to the deformation along the sensitivity vector can be calculated from two interferograms of the object, one in its undeformed and one in its deformed state.

With respect to the off-axis methods described in Refs. 3–6 (in which a constant carrier frequency along one axis was used), the method described in this paper has some advantages and some disadvantages. The wave fields are well separated in the off-axis hologram; this allows easier filtering of the unwanted wave fronts. In the in-line arrangement separation is obtained by reconstruction of the focused and the defocused images in different planes. The disadvantage of the in-line method is the variation of carrier frequency over the image. At the center we have low carrier frequencies, and at the border we have high carrier frequencies. This produces results of low quality at the center of the image. We have shown that this problem can be solved by using both the primary and the conjugate reconstructions. The other disadvantage is that the evaluation of each hologram involves four Fourier transforms and thus a longer evaluation time (with a PC computer with a Pentium 100-MHz processor, a Fourier transform of an array with 512×512 points can be carried out in 10 s).

The in-line method has the advantage that a circular aperture with larger surface than that in the method described in Ref. 3 can be used. A large aperture means a higher spatial resolution (smaller speckle) and higher light intensity on the CCD chip. This permits the use of lasers with lower energy. It should be noted that, by increasing the aperture size, we increase the noise as well, but we have shown that

the phase map obtained still has good quality, even when large apertures are used. Using a circular aperture results in the speckle on the CCD having the same extension in the x and the y directions; with a rectangular aperture (see Ref. 3) the speckle extension in one direction is larger than in the other.

The optical arrangement (Fig. 1) used is very simple, and alignment is not critical. In particular, it is not necessary that the point source and the center of the aperture be located exactly on the z axis. If the arrangement is not perfectly in line, we obtain by digital reconstruction the aperture shifted with respect to the center. In this case it is necessary only to shift the filter to select reconstruction of the image of the aperture; the other operations necessary to determine the phase do not change.

For in-line digital holography it is possible to use arrangements that are different from that shown in Fig. 1. In particular, it is not necessary for the point source of the reference to be located in the front focal plane of the imaging lens. It is necessary only that the reference point and the aperture be in different planes to produce a carrier frequency. The carrier frequency permits the separation of twin images. The condition describing the higher recordable spatial frequency [relation (6)] should be satisfied. The best separation between twin images was obtained when $(d - b) = [(2N_x + 2N_y + 2)\Delta^2]/\lambda$.

In-line, digital, lensless Fresnel holograms could be recorded as well; in this case the arrangement to be used is similar to those described in Refs. 5 and 6 for off-axis holograms. The only difference is that the reference and the object beams propagate in the same direction but have the different curvatures necessary for separation of the twin reconstructions.

References

1. C. M. Vest, *Holographic Interferometry* (Wiley, New York, 1979).
2. R. Jones and C. Wikes, *Holographic and Speckle Interferometry*, 2nd ed., Vol. 6 of Cambridge Studies in Modern Optics (Cambridge U. Press, Cambridge, 1989).
3. G. Pedrini, H. Tiziani, and Y. Zou, "Digital double-pulse TV-holography," Opt. Laser Eng. **26,** 199–219 (1997).
4. M. Takeda, I. Hideki, and S. Kobayashi, "Fourier-transform method of fringe-pattern analysis for computer-based topography and interferometry," J. Opt. Soc. Am. **72,** 156–160 (1982).
5. U. Schnars, "Direct phase determination in hologram interferometry with use of digitally recorded holograms," J. Opt. Soc. Am. A **11,** 2011–2015 (1994).
6. G. Pedrini, Y. L. Zou, and H. J. Tiziani, "Digital double-pulse holographic interferometry for vibration analysis," J. Mod. Opt. **42,** 367–374 (1995).
7. R. J. Collier, C. B. Burckhard, and L. H. Lin, *Optical Holography* (Academic, New York, 1971).
8. M. Adams, T. Kreis, and W. Juptner, "Particle size and position measurement with digital holography," in *Optical Inspection and Measurements II*, C. Gorecki, ed., Proc. SPIE **3098,** 234–240 (1997).
9. L. Onural and P. D. Scott, "Digital decoding of in-line holograms," Opt. Eng. **26,** 1124–1132 (1987).